Asian Journal of Chemistry; Vol. 29, No. 9 (2017), 2005-2010

ASIAN JOURNAL OF CHEMISTRY

https://doi.org/10.14233/ajchem.2017.20726

X-Ray Analysis of Cadmium Oxide Nanostructured Films Synthesized with Different Precursor Molarities by Silar Method

HITEN SARMA[1,*], DHRUBA CHAKRABORTTY[2] and K.C. SARMA[1]

[1]Department of Instrumentation & USIC, Gauhati University, Guwahati-781 014, India
[2]Department of Chemistry, B.N. College, Dhubri-783 324, India

*Corresponding author: E-mail: hitensarma7@gmail.com; ritul1967@rediffmail.com

Received: 24 April 2017; *Accepted*: 29 May 2017; *Published online*: 15 July 2017; AJC-18484

Nanostructured cadmium oxide thin films have been synthesized onto suitably cleaned glass substrates by SILAR (successive ionic layer adsorption and reaction) method. X-ray diffraction study confirms the formation of nanocrystalline cubic phase of cadmium oxide in the films. Lattice constant is determined using Nelson Riley plots. Using X-ray broadening, crystallite sizes, lattice strain, stress and energy density were studied by using Williamson-Hall method and modified Williamson-Hall method. From literature review, it is seen that a number of researchers have applied these two methods for structural characterization of thin films of different nanocrystals, but till now modified Williamson-Hall method has not been used for CdO nanocrystals. Hence, we have used these methods for structural characterization of deposited CdO thin films. The ultra-high resolution transmission electron microscopic (UHRTEM) study shows that the shape of the particles is nearly spherical and the average particle size agrees well with the result obtained from X-ray diffraction study. Selected area electron diffraction patterns have also supported the formation of cubic phase of cadmium oxide.

Keywords: Cadmium oxide thin films, Williamson-Hall plot, Nelson-Riley plot, Size-strain plot.

INTRODUCTION

Nanostructured materials have drawn attentions to the researchers due to the unique physical and chemical properties of nanomaterials, which are different from those of either the bulk materials or single atoms [1]. The reduction of the size of materials causes a deviation of their physical and chemical properties from the bulk and such resultant materials (nanoparticles) are known to possess potential applications and novel properties [2]. Among the different metal oxide films, CdO is an important n-type semiconductor with a cubic structure, which belongs to the II–VI group, with a direct band gap of 2.5 eV and indirect band gap 1.98 eV [3]. Up to now, various methods have been employed to prepare the cadmium oxide nanostructures such as hydrothermal method [4], microwave-assisted combustion method [5], solvothermal method [6], chemical co-precipitation method [7], vapour phase transport [8], thermal evaporation [9], sonochemical method [10] and mechano chemical method [11]. We have used SILAR (successive ionic layer adsorption and reaction) technique for the preparation of thin films which is presently attracting considerable attention, as it does not require sophisticated instrumentation like vacuum system and other expensive equipment. Simple equipment like hot plate with magnetic stirrer is needed for this method [12].

Nelson Riley plot has been used by many research groups for calculating the lattice constant of a cubic system [13,14]. We have also used it for the same purpose. Crystallite size, lattice strain and stress have been calculated using Williamson-Hall method, modified Williamson-Hall method and uniform deformation energy density model [15-17]. Size-strain plot (SSP) have also been used for finding size and strain of the prepared films [14,18,19], which is also used here. As far our best of knowledge modified Williamson-Hall method for structural characterization is used mainly for CdS, PbS, ZnO, *etc.* nanostructures and detailed application of modified Williamson-Hall method for CdO nanostrucured is not shown yet. Hence we have used application of modified Williamson-Hall method for structural characterization of synthesized CdO films.

EXPERIMENTAL

Cleaning of the substrate: The microscope glass substrate was cleaned with following steps (1) washed with mild detergent, (2) rinsed with distilled water, (3) dipped in dilute chromic acid for 3 h (4) rinsed thoroughly with distilled water and (5) heated at 20 °C for 10 min by keeping the substrate vertically.

Cadmium nitrate hexahydrate, sodium hydroxide were purchased from Merck and were used as received since they

were of analytical reagent grade with 99 % purity. Double distilled water was used for all procedures of sample preparation and dilution.

Deposition of thin film: Cadmium oxide thin films were deposited onto the cleaned glass substrates by alternate immersion of the glass substrate in $Cd(NO_3)_2$ (Cd^{2+} ion source) and in double distilled water (OH^- source) at room temperature. Cadmium nitrate and H_2O served as the cationic and anionic solutions respectively. The alkalinity of cadmium nitrate solution was increased to pH ~12 with the addition of sodium hydroxide. As the cleaned glass substrate was immersed in the alkaline cadmium nitrate solution, cadmium complex adsorbed on the substrate. The glass substrate with the cadmium complex is then immersed in distilled water and the reaction occurred on the glass surface to form $Cd(OH)_2$. The period of dipping the substrate in the cadmium bath (30 s) was referred as ''adsorption'' and that in H_2O (15 s) as ''reaction''. This process forms one cycle and was repeated 50 times in order to increase the film thickness. After each cycle, the glass slide was rinsed with distilled water and after a complete cycle the films were dried with an air dryer. Finally, the deposited films were annealed in air at 350 °C for 2 h to transform the hydroxide phase to the oxide. The precursor solutions were prepared by adding $Cd(NO_3)_2$ solutions of 0.25, 0.50 and 0.75 molar concentrations separately to an aqueous solution of 2 M NaOH under a high stirring rate (200 rpm) condition. During the stirring process a constant temperature 30 °C was maintained for 3 h.

Mechanism of thin film formation: Dipping the glass slides in the beaker containing cadmium nitrate and excess sodium hydroxide solution causes a cadmium complex ion to adsorb on the substrate due to attractive forces between ions in the solution and that on the glass. Atoms or molecules of glass surface possess unbalanced or residual force and hold the substrate particles. The cadmium complex ions can be represented with the following equations:

$$Cd(NO_3)_2 + 2NaOH \longrightarrow Cd(OH)_2 + 2NaNO_3$$

$$Cd(OH)_2 + NaOH \longrightarrow Na(Cd)(O)^{2-} + H_2O + 2H^+$$

The glass substrate with the adsorbed cadmium sodium oxide ion is immersed into a beaker of distilled water and the ion is converted into cadmium hydroxide. Sodium ion in the complex is attracted to the hydroxide ion to form sodium hydroxide while the CdO^{2-} in the complex is attracted to the H^+ to form the cadmium hydroxide ion.

$$(Na)CdO^{2-} + H_2O \longrightarrow Cd(OH)^{2-} + NaOH$$

$$Cd(OH)^{2-} + heat \longrightarrow CdO + H_2O$$

On annealing at a temperature of 350 °C the cadmium hydroxide transforms into the cadmium oxide phase. The deposited films showed good adherence to the substrate after annealing.

RESULTS AND DISCUSSION

X-ray diffraction structural analysis: X-ray diffraction patterns of CdO samples were recorded in PANalytical X'Pert Pro XRD with CuK_α radiation (k = 1.54056 Å) at room temperature. Surface morphology was analyzed by ultrahigh resolution transmission electron microscope (UHRTEM) (JEM 2100) operated at 200 kV.

X-ray diffraction pattern of CdO films calcined at 350 °C is shown in Fig. 1. The sharp and well defined peaks confirm a face centered cubic (fcc) structure of CdO. The inter-planar spacing (d) [calculated from the Bragg equation (eqn. 2)] and lattice constant (a) (calculated from eqn. 1 for cubic phase structure) of CdO-films samples with different molarities were determined which is very close to the reported values (JCPDS, No. 05-0640).

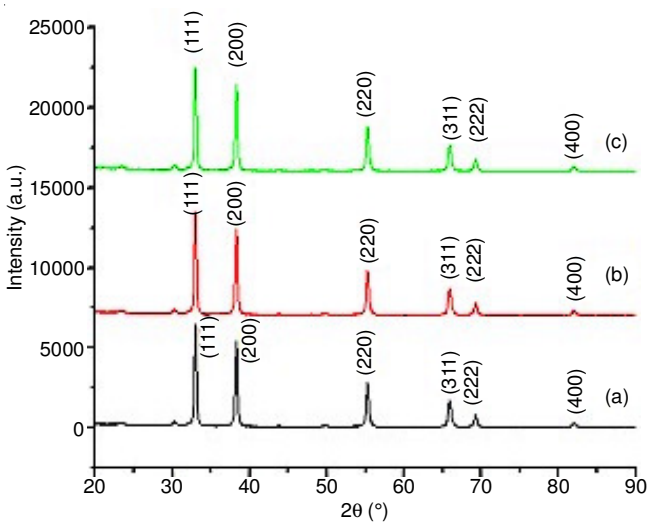

Fig. 1. XRD Patterns of CdO films with molarities (a) 0.25 M, (b) 0.50 M and (c) 0.75 M

Lattice constant: The lattice constant 'a' for the cubic phase structure is determined by the relation:

$$a = d\,(h^2 + k^2 + l^2)^{1/2} \quad (1)$$

where 'd' is the interplanar spacing of the crystal planes represented by Miller Indices (h k l) and is given by

$$\lambda = 2d \sin\theta \quad (2)$$

The corrected values of lattice constants are estimated from the Nelson-Riley plots. The Nelson-Riley curve is a plot between the calculated 'a' for different planes and error function [20] given by

$$f(\theta) = \frac{1}{2}\left(\frac{\cos^2\theta}{\sin\theta} + \frac{\cos^2\theta}{\theta}\right) \quad (3)$$

and extrapolation to θ = 90º. A typical Nelson-Riley plot for synthesized samples are shown in Fig. 2 and values are shown in Table-1. The lattice constant 'a_{corr}' of the film calculated using Nelson-Riley plot (Table-1) is different from its bulk value a_o which is 4.696 Å. This means the particles are under strain which contributes towards broadening of the diffraction peak. It is clear from the Fig. 1 that all peaks corresponds to fcc structure of CdO and no other impurity peaks are found.

Crystallite size: Crystallite size of the prepared CdO-Films is estimated from the Scherrer's formula [21]:

$$\beta_D = \frac{\kappa\lambda}{D\cos\theta} \quad (4)$$

where the constant K is taken as 0.9, λ is the wavelength of the wavelength of X-rays used (λ = 1.5406 Å), β_D is the full width at half maximum of the diffraction peaks.

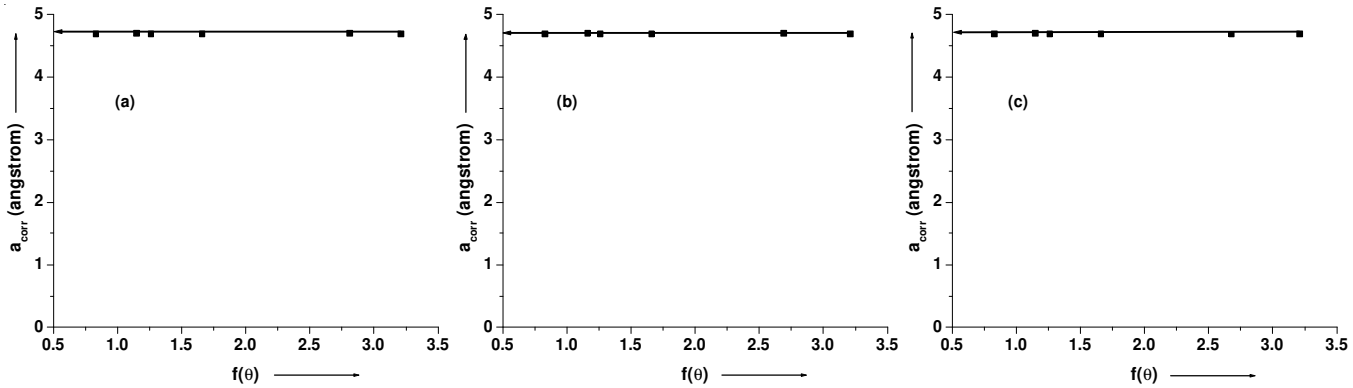

Fig. 2. Nelson-Riley plots of CdO films for (a) 0.25 M, (b) 0.50 M and (c) 0.75 M

TABLE-1
STRUCTURAL PARAMETERS OF CHEMICALLY DEPOSITED CdO FILMS WITH DIFFERENT MOLARITIES

Molarity (M)	d (Å)	hkl	FWHM β (°)	2θ (°)	a_{calc} (Å)	a_{corr} (Å)
0.25	2.711	111	0.261	32.99	4.695	4.694
	2.347	200	0.288	38.29	4.700	
	1.659	220	0.355	55.28	4.692	
	1.415	311	0.406	65.92	4.693	
	1.356	222	0.413	69.25	4.697	
	1.173	400	0.466	82.02	4.692	
0.50	2.711	111	0.227	33.03	4.695	4.695
	2.347	200	0.241	38.32	4.694	
	1.659	220	0.294	55.31	4.692	
	1.415	311	0.324	65.94	4.693	
	1.356	222	0.329	69.27	4.697	
	1.174	400	0.379	82.03	4.698	
0.75	2.711	111	0.206	33.08	4.695	4.694
	2.340	200	0.222	38.37	4.680	
	1.659	220	0.270	55.36	4.692	
	1.415	311	0.312	65.99	4.693	
	1.356	222	0.317	69.32	4.697	
	1.174	400	0.345	82.09	4.696	

Williamson-Hall method: In X-ray diffraction, the broadening of XRD line profile is not only due to crystallite size but also due to the presence of non-uniform strain in the material. If the size and strain broadening is present simultaneously then crystallite size and strain may be found from Williamson-Hall plot.

Crystal imperfections and distortion of strain induced peak broadening are related by:

$$\varepsilon = \frac{\beta_S}{4\tan\theta} \Rightarrow \beta_S = 4\varepsilon\tan\theta \quad (5)$$

Depending on different 'θ' positions, the separation of size and strain broadening analysis is done using Williamson-Hall method:

$$\beta = \beta_S + \beta_D \quad (6)$$

Substituting eqns. 4 and 5 in the above equation we get,

$$\beta = \frac{\kappa\lambda}{D\cos\theta} + 4\varepsilon\tan\theta$$

$$\Rightarrow \beta\cos\theta = \frac{\kappa\lambda}{D} + 4\varepsilon\sin\theta \quad (7)$$

Eqn. 7 represents the uniform deformation model (UDM). Here the strain is assumed to be uniform in all crystallographic directions. The breadth of Bragg peak is a combination of both instrument and sample dependent effects. To decouple these contributions, it is necessary to collect a diffraction pattern from the line broadening of a standard material such as silicon to determine the instrumental broadening. The instrumental broadening corrected FWHM (β) of each reflection is calculated using the following equation [22]

$$\beta^2 = (\beta)^2_{measured} - (\beta)^2_{instrumental} \quad (8)$$

A graph is drawn with 4 sin θ along X-axis and β cos θ along Y-axis (Fig. 3). From the graph, strain and crystallite size are calculated from the slope and y intercept of the fitted line respectively and the values are tabulated in Table-2. It is observed that there is a gradual increase in crystallite size obtained both from Scherrer's formula and Williamson-Hall plot with the increase in the molarities of the solutions [Fig. 4(a) and 4(b)]. A similar kind of result has been also reported earlier by other workers [23]. There is a decrease in strain with molarity [Fig. 4(c)].

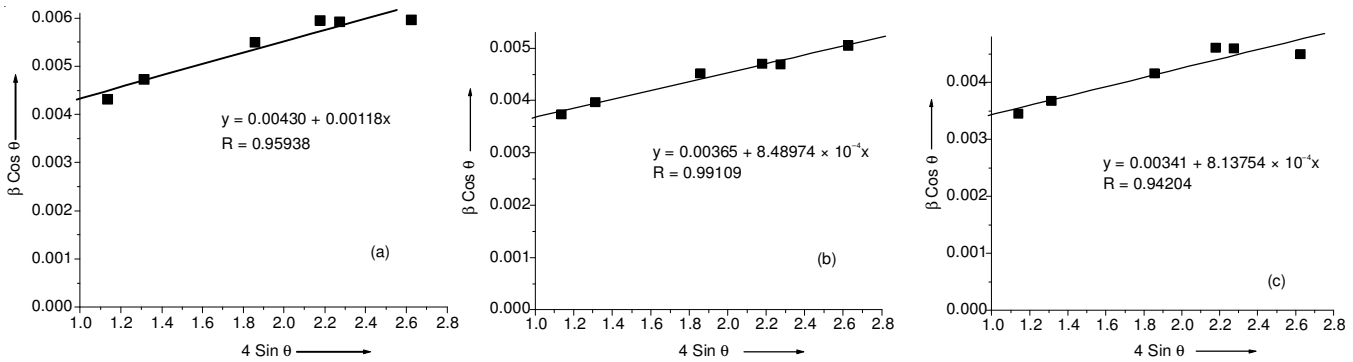

Fig. 3. Williamson-Hall plots of CdO films for (a) 0.25 M, (b) 0.50 M and (c) 0.75 M

TABLE-2
GEOMETRIC PARAMETERS OF PREPARED CdO FILMS USING W-H METHOD & MODIFIED W-H METHOD

Molarity of solution (M)	Scherrer method	Williamson method								
		UDM		USDM			UDEDM			
	D (nm)	D (nm)	Strain $\varepsilon \times 10^{-3}$	D (nm)	Strain $\varepsilon \times 10^{-3}$	Stress σ (MPa)	D (nm)	Strain $\varepsilon \times 10^{-3}$	Stress σ (MPa)	u (KJ/m^3)
0.25	30.02	33.66	1.180	34.55	1.087	158.34	34.55	1.136	165.58	94.09
0.50	35.49	39.66	0.849	40.32	0.933	136.02	40.89	0.822	119.76	49.28
0.75	38.78	42.45	0.814	43.60	0.741	108.01	42.45	0.779	113.50	44.22

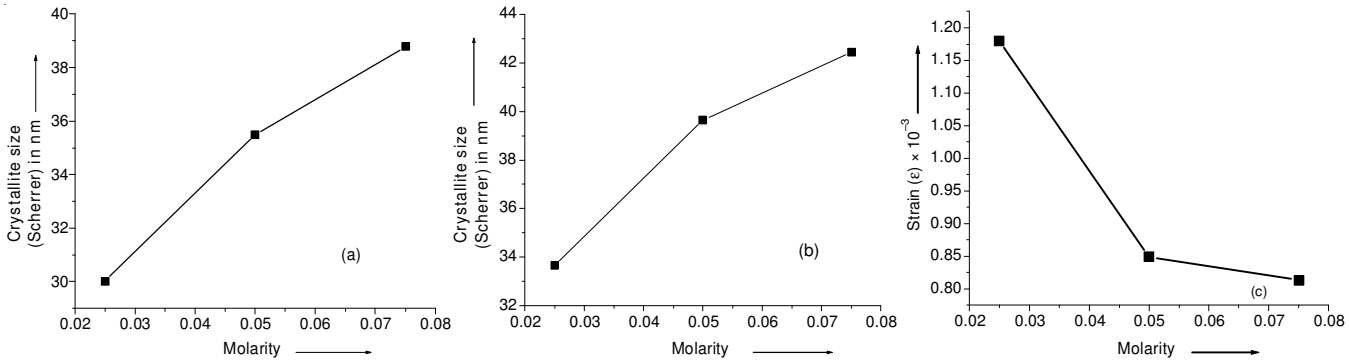

Fig. 4. (a) Crystallite size from Scherrer's formula *versus* molarity. (b) Crystallite size from Williamson-Hall plot *versus* molarity. (c) Strain from Williamson-Hall plot *versus* molarity of CdO

Size-strain plot method: Size–strain plot' (SSP) can be used for estimation of size–strain parameters for isotropic line broadening. In this method, less importance is given to the data from reflection at high angles, because, normally precision is less in those ranges of angles [24]. In this approximation method, the "crystallite size" profile is described by a Lorentzian function and the "strain profile" is described by Gaussian function [25]. Then one can write:

$$\left(\frac{d\beta\cos\theta}{\lambda}\right)^2 = \frac{1}{D}\left(\frac{d^2\beta\cos\theta}{\lambda}\right) + \left(\frac{\varepsilon}{2}\right)^2 \quad (9)$$

The term $\left(\frac{d^2\beta\cos\theta}{\lambda}\right)$ is plotted along X-axis against $\left(\frac{d\beta\cos\theta}{\lambda}\right)^2$ along Y-axis for different peak orientations of 0.25, 0.50 and 0.75 M of CdO films as shown in Fig. 5(a)–5(c). The crystallite size is determined from the slope of the linearly fitted data and the value of strain is obtained from y-intercept. The size of the crystallite is obtained from $D = \frac{k\lambda}{\text{slope}}$ where K = 3/4 for spherical particle. The mean apparent strain is $\varepsilon_{app} = 2\left(\sqrt{\text{y intercept}}\right)$ and the root mean square strain is obtained from relation [26] $\varepsilon = \frac{\varepsilon_{app}}{2\pi\sqrt{2}}$. The estimated values of D and ε are shown in Table-3.

TABLE-3
GEOMETRIC PARAMETERS OF CdO FILMS
PREPARED USING SIZE-STRAIN PLOT METHOD

Molarity of solution (M)	D (nm)	Strain $\varepsilon \times 10^{-3}$
0.25	49.36	1.009
0.50	53.22	0.766
0.75	59.23	0.751

Modified Williamson-Hall method: From uniform stress deformation model (USDM), strain is calculated from Hooke's law maintaining linear proportionality between stress and strain given by $\sigma = Y\varepsilon$ where σ is the stress, ε is the strain and Y is the Young's modulus. Applying Hooke's law approximation to eqn. 7, we get:

$$\beta\cos\theta = \frac{k\lambda}{D} + \frac{4\sigma}{Y}\sin\theta \quad (10)$$

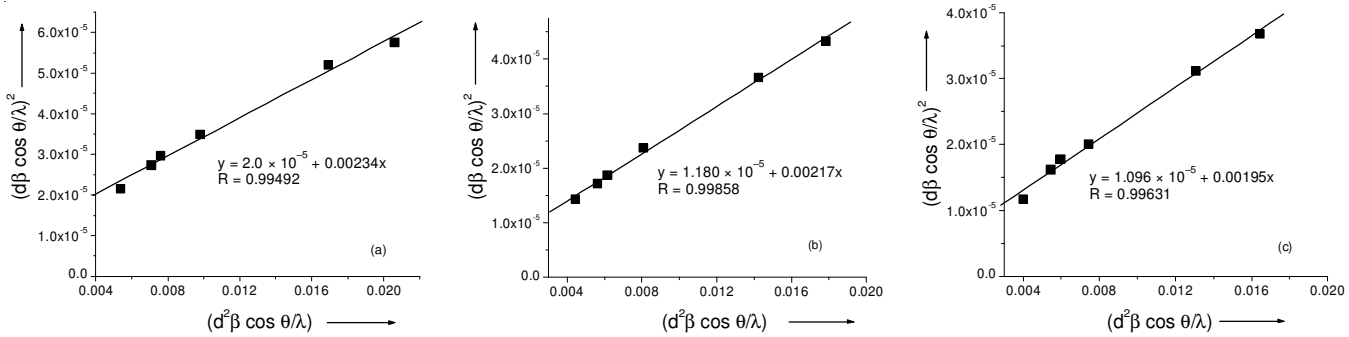

Fig. 5. Size–strain plots of CdO films for (a) 0.25 M, (b) 0.50 M and (c) 0.75 M

Again, the modulus of elasticity or Young's modulus 'Y' for cubic crystal is given by the relation [27]:

$$\frac{1}{Y} = S_{11} - 2\left(S_{11} - S_{12} - \frac{1}{2}S_{44}\right)\frac{(hk)^2 + (hl)^2 + (kl)^2}{(h^2 + k^2 + l^2)^2} \quad (11)$$

where S_{11}, S_{12}, S_{44} are the elastic compliances of CdO. The relation connecting elastic compliances and the stiffness C_{ij} are as follows [28]:

$$S_{11} = \frac{C_{11} + C_{12}}{(C_{11} - C_{12})(C_{11} + 2C_{12})} \quad (12)$$

$$S_{12} = -\frac{C_{12}}{(C_{11} - C_{12})(C_{11} + 2C_{12})} \quad (13)$$

and

$$S_{44} = \frac{1}{C_{44}} \quad (14)$$

Using the values of C_{11}, C_{12} and C_{44} [29] as 207.8 GPa, 106.3 GPa and 54.9 GPa respectively, we can calculate elastic compliances S_{11}, S_{12}, S_{44} which are given as 7.36×10^{-12}, -2.49×10^{-12} and 18.21×10^{-12} m^2/N respectively. Young's modulus Y has been calculated and resulted to be 145.7 GPa for (111) lattice plane followed by Y = 135.9 GPa for (200), Y = 143.1 GPa for (220), Y = 140.3 GPa for (311), Y = 145.69 GPa for (222) and Y = 135.9 GPa for (400) lattice planes, respectively. A graph is plotted between 4 sinθ/Y along X-axis and βcosθ along Y-axis (Fig. 6). The stress is calculated from the slope of the graph and crystallite size from the Y intercept and the values are presented in Table-2. The energy density of a crystal was calculated from a model called uniform deformation energy density model (UDEDM). According to Hooke's law, the energy density u (energy per unit volume) is $u = \frac{\varepsilon^2 Y}{2}$. Therefore, eqn. 7 can be modified to the form:

$$\beta\cos\theta = \frac{\kappa\lambda}{D} + 4\sin\theta\left(\frac{2u}{Y}\right)^{1/2} \quad (15)$$

A graph is plotted between $4\sin\theta\left(\frac{2}{Y}\right)^{1/2}$ along X -axis and β cos θ along Y-axis (Fig. 7). From the slope of the graph, energy density u is calculated and the crystallite size D is calculated from the Y intercept and the values are tabulated in Table-2.

Transmission electron microscopy: The UHRTEM micrograph of CdO sample of 0.50 molarity is shown in Fig. 8(a). The image of CdO sample shows the presence of large number of nearly spherical CdO nanoparticles. The shapes of the particles are nearly spherical and obviously demonstrate aggregation of the particles. The aggregation of particles should had been originated from the large specific surface area and high surface energy of CdO nanoparticles [30]. The aggregation occurred probably during the process of drying [31,32]. The average particle size of the CdO sample is found to be 50 nm, which is very nearly close to the result obtained based on XRD study (53.22 nm) by SSP method. Fig. 8(b) shows selected area electron diffraction (SAED) pattern of the sample consisting of a central halo and concentric rings, which indicate the crystalline structure of the sample. The well crystallinity can be observed in lattice planes along (111), (200) and (220) having values of d (nm) (interplanar spacing of the crystal planes) as 0.275, 0.235 and 0.166 respectively [Fig. 8(b)] and the selected area diffraction pattern (SAED) is shown in inset [Fig. 8(c)].

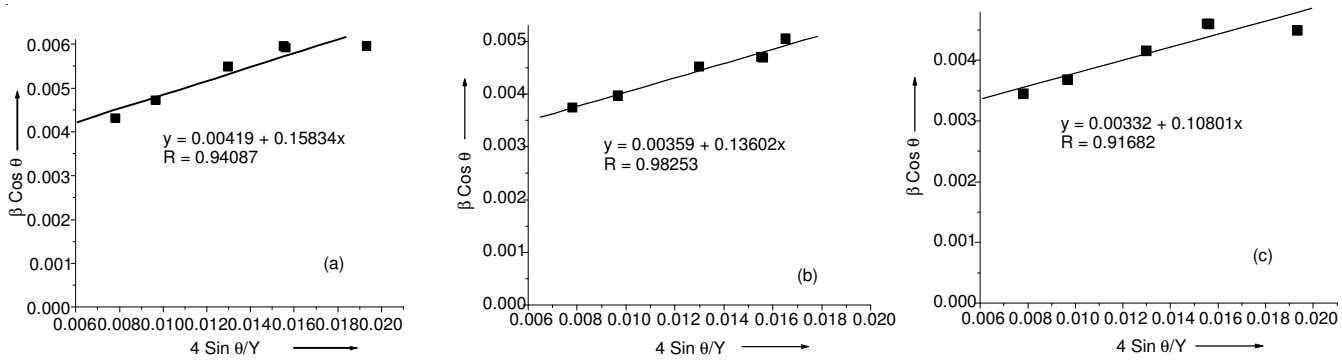

Fig. 6. Modified Williamson-Hall plots of CdO films for (a) 0.25 M, (b) 0.50 M and (c) 0.75 M

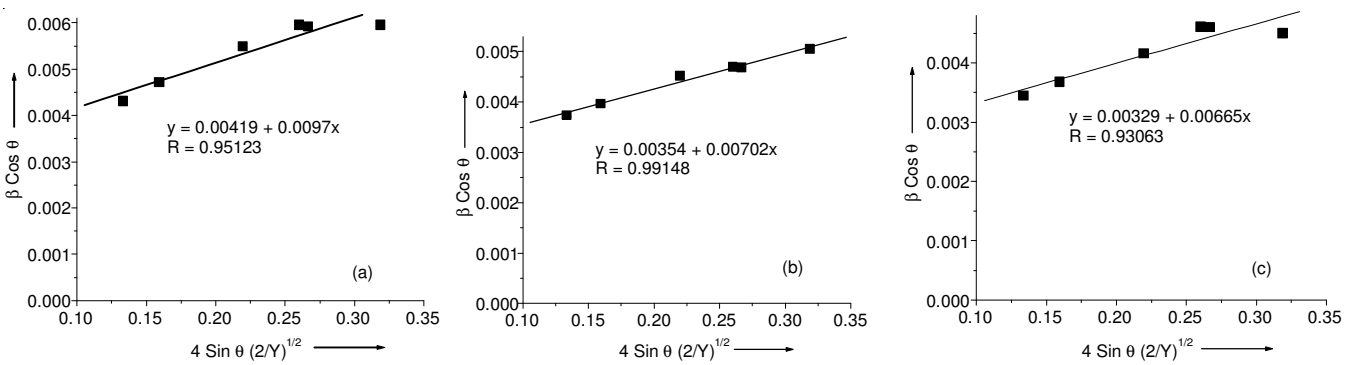

Fig. 7. Uniform deformation energy density model plot of CdO films for (a) 0.25 M, (b) 0.50 M and (c) 0.75 M

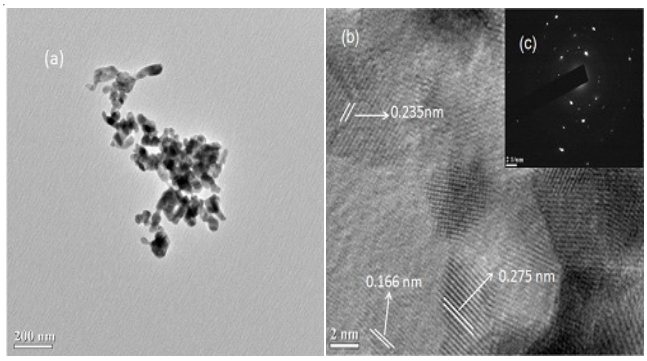

Fig. 8. (a) TEM micrograph of CdO sample with 0.50 M (b) lattice planes and (c) SAED pattern of CdO of molarity 0.50 M (inset)

Conclusion

Nanostructured CdO films deposited by SILAR method are found to be uniform and have good adherence to the substrates. The formation of CdO nanoparticles have been confirmed by XRD and HRTEM analyses. The peak broadening was analyzed by the Scherrer's equation, SSP and modified forms of Williamson-Hall models *viz.* UDM, USDM and UDEDM. Among Williamson-Hall methods, UDM considers the homogeneous isotropic nature of the crystal where as USDM and UDEDM models consider the anisotropic nature of the crystallites. The average values of crystallite size obtained from UDM, USDM and UDEDM are almost similar which indicate the inclusion of strain in various forms of Williamson-Hall analysis has some effect on the average crystallite size of CdO nanoparticles. Some variation in the average crystallite size obtained from Scherrer's formula and Williamson-Hall analysis was due to the difference in averaging the particle size distribution. The above-explained methods were helpful in determining the crystallite size, strain, stress and energy density value and among them SSP method is highly preferable to define the crystal perfection. From different models and methods, it is seen that with the increase in molar concentration of the precursor solutions strain, stress and energy density of the nanocrystals decrease, whereas crystallite size of the prepared CdO films increases.

ACKNOWLEDGEMENTS

The authors would like to thank SAIF, Gauhati University, Guwahati, India for XRD analysis and also thankful to SAIF, NEHU, Shillong, India for TEM analysis.

REFERENCES

1. V.S. Muralidharan and A. Subramania, Nanoscience and Technology, CRC Press, New Delhi, pp. 542 (2009).
2. B.C. Ejelonu and P.A. Ajibade, *Chalcogenide Lett.*, **13**, 563 (2016).
3. D.R. Lide, CRC Handbook of Chemistry and Physics, CRC Press, Boca Raton, edn 77, p. 12/97 and 3/278 (1996/97).
4. F. Zhang, F. Bei, J. Cao and X. Wang, *J. Solid State Chem.*, **181**, 143 (2008); https://doi.org/10.1016/j.jssc.2007.11.004.
5. N.C.S. Selvam, R.T. Kumar, K. Yogeenth, L.J. Kennedy, G. Sekaran and J.J. Vijaya, *Powder Technol.*, **211**, 250 (2011); https://doi.org/10.1016/j.powtec.2011.04.031.
6. N. Varghese, L.S. Panchakarla, M. Hanapi, A. Govindaraj and C.N.R. Rao, *Mater. Res. Bull.*, **42**, 2117 (2007); https://doi.org/10.1016/j.materresbull.2007.01.017.
7. D.D. Vijaykarthik, M. Kirithika, N. Prithivikumaran and N. Jeyakumaran, *Int. J. Nano Dimens.*, **5**, 557 (2014); https://doi.org/10.7508/ijnd.2014.06.007.
8. T. Kuo and M.H. Huang, *J. Phys. Chem. B*, **110**, 13717 (2006); https://doi.org/10.1021/jp062854x.
9. H.B. Lu, L. Liao, H. Li, Y. Tian, D.F. Wang, J.C. Li, Q. Fu, B.P. Zhu and Y. Wu, *Mater. Lett.*, **62**, 3928 (2008); https://doi.org/10.1016/j.matlet.2008.05.010.
10. A. Askarinejad and A. Morsali, *Mater. Lett.*, **62**, 478 (2008); https://doi.org/10.1016/j.matlet.2007.05.082.
11. A. Tadjarodi and M. Imani, *Mater. Lett.*, **65**, 1025 (2011); https://doi.org/10.1016/j.matlet.2010.12.054.
12. A. Ivanauskas, R. Ivanauskas and I. Ancutiene, *Chalcogenide Lett.*, **13**, 373 (2016).
13. N. Choudhury and B.K. Sarma, *Bull. Mater. Sci.*, **32**, 43 (2009); https://doi.org/10.1007/s12034-009-0007-y.
14. P.K. Mochahari and K.C. Sarma, *Indian J. Phys.*, **88**, 1265 (2014); https://doi.org/10.1007/s12648-014-0590-7.
15. V.D. Mote, Y. Purushotham and B.N. Dole, *J. Theor. Appl. Phys.*, **6**, 6 (2012); doi:10.1186/2251-7235-6-6.
16. Y.T. Prabhu, K.V. Rao, V.S. Kumar and B.S. Kumari, *World J. Nano Sci. Eng.*, **4**, 21 (2014); https://doi.org/10.4236/wjnse.2014.41004.
17. P. Triloki, P. Garg, R. Rai and B.K. Singh, *Nucl. Instrum. Methods Phys. Res. A*, **736**, 128 (2014); https://doi.org/10.1016/j.nima.2013.10.075.
18. P.K. Mochahari, A. Rajbongshi, N. Choudhury, F. Singh and K.C. Sarma, *Adv. Mater. Lett.*, **6**, 354 (2015); https://doi.org/10.5185/amlett.2015.5719.
19. P.K. Mochahari and K.C. Sarma, *Indian J. Phys.*, **90**, 21 (2016); https://doi.org/10.1007/s12648-015-0721-9.
20. J.B. Nelson and D.P. Riley, *Proc. Phys. Soc. Lond.*, **57**, 160 (1945); https://doi.org/10.1088/0959-5309/57/3/302.
21. S. Sen, S. K. Halder and S. P. Sen Gupta, *J. Phys. Soc. Jpn.*, **38**, 1641 (1975); https://doi.org/10.1143/JPSJ.38.1641.
22. K.D. Rogers and P. Daniels, *Biomaterials*, **23**, 2577 (2002); https://doi.org/10.1016/S0142-9612(01)00395-7.
23. V. Saravanan, J. Joseph Prince and M. Anusuya, *APRN J. Eng. Appl. Sci.*, **10**, 2453 (2015).
24. A.K. Zak and W.H.A. Majid, *Ceram. Int.*, **36**, 1905 (2010); https://doi.org/10.1016/j.ceramint.2010.03.022.
25. M.A. Tagliente and M. Massaro, *Nucl. Instrum. Methods Phys. Res. B*, **266**, 1055 (2008); https://doi.org/10.1016/j.nimb.2008.02.036.
26. P. Rageswari and S. Dhanuskodi, *Cryst. Res. Technol.*, **48**, 589 (2013); https://doi.org/10.1002/crat.201300102.
27. J.-M. Zhang, Y. Zhang, K.-W. Xu and V. Ji, *Mater. Lett.*, **62**, 1328 (2008); https://doi.org/10.1016/j.matlet.2007.08.038.
28. A.A. Kelly and K.M. Knowles, Crystallography and Crystal Defects, Wiley, edn 2 (2012).
29. A.J. Cinthia, G. Sudhapriyang, R. Rajeswarapalanichamy and M. Santhosh, *Procedia Mater. Sci.*, **5**, 1034 (2014); https://doi.org/10.1016/j.mspro.2014.07.394.
30. D. Raoufi, *J. Lumin.*, **134**, 213 (2013); https://doi.org/10.1016/j.jlumin.2012.08.045.
31. R.Y. Hong, J.Z. Qian and J.X. Cao, *Powder Technol.*, **163**, 160 (2006); https://doi.org/10.1016/j.powtec.2006.01.015.
32. R.Y. Hong, J.H. Li, L.L. Chen, D.Q. Liu, H.Z. Li, Y. Zheng and J. Ding, *Powder Technol.*, **189**, 426 (2009); https://doi.org/10.1016/j.powtec.2008.07.004.